

## Reviewer 2 response

The authors wish to thank the referee for their time and effort in reviewing the manuscript. The comments and suggestions have helped us to improve the quality of the work and clarify important points in the discussion. Our responses to the comments are included below.

### Main comments

1. **The pressure Poisson equation neglects streamwise derivatives. This appears to be a major limitation, as it will not correctly resolve the induced velocity in the streamwise direction which is critical to predict the power production and the wake velocity at the outlet of the inviscid streamtube. The authors should calculate the resolved induction in their model and compare it to LES. Also the maximum wake velocity as a function of  $x$  should be plotted from  $x/D=-5$  to 15 for each single turbine LES case and model.**

In the formulation of the pressure Poisson equation, we should note that only the *second* derivatives in  $x$  are neglected, while the first order derivatives are still retained in the right hand side forcing term. This maintains consistency with the parabolization approach, where quantities are assumed to vary sufficiently slowly in the streamwise direction that derivatives such as  $\frac{\partial^2 u}{\partial x^2}$ ,  $\frac{\partial^2 p}{\partial x^2}$ , etc., can be ignored relative to the gradients  $\frac{\partial u}{\partial x}$ ,  $\frac{\partial p}{\partial x}$ ,  $\frac{\partial u}{\partial z}$ ,  $\frac{\partial p}{\partial z}$ , etc. As formulated, streamwise pressure influences are still allowed, but only in the *downstream* direction. Parabolized versions of the Navier-Stokes equations have been successfully applied in many contexts, including boundary layers, mixing layers and jets, and can capture complex phenomena such as vortex roll-up and pairing (see the study of [4]).

This parabolization process removes elliptic influences from the system, so that the solution can be determined by marching in the streamwise direction. However, as the reviewer notes, the effects of turbine induction are explicitly excluded from this formulation. In cases where turbines are sufficiently close to lie in neighboring induction zones, or where flow acceleration between turbines can be affect the wake behavior, the effects of turbine blockage can be included by superimposing an induction field on top of the RANS solution. The work of Cheung et al [3] contains an example of such a calculation using a Green's function approach and an inflow profile, and can be adapted to the current situation. The development of such a method is a matter of ongoing research, and worthy of study in detail.

As discussed in question 11 below, the updated manuscript contains a description of the wake skew as a function of the streamwise distance, which may be more relevant to the current study of wake and veer interactions. For the single turbine cases, upstream wake profiles remain unchanged (see the discussion in question 5 below).

2. **ABL physics inconsistency: A substantial portion of this paper focuses on veer effects, but the presented equations neglect Coriolis forces which are**

largely responsible for veer. The authors also use a turbulence model that is for surface layer, which neglects Coriolis forces and veer.

In the updated manuscript, we have clarified that the inflow profiles based on Monin-Obukhov theory are applicable to the atmospheric surface layer. The governing equations have also been updated to include the Coriolis body forces:

$$u \frac{\partial u}{\partial x} + v \frac{\partial u}{\partial y} + w \frac{\partial u}{\partial z} = -\frac{1}{\rho} \frac{\partial p}{\partial x} + \frac{\partial}{\partial y} \left( (\nu + \nu_T) \frac{\partial u}{\partial y} \right) + \frac{\partial}{\partial z} \left( (\nu + \nu_T) \frac{\partial u}{\partial z} \right) + f_{T,x} + f_{COR,x} \quad (2a)$$

$$u \frac{\partial v}{\partial x} + v \frac{\partial v}{\partial y} + w \frac{\partial v}{\partial z} = -\frac{1}{\rho} \frac{\partial p}{\partial y} + \frac{\partial}{\partial y} \left( (\nu + \nu_T) \frac{\partial v}{\partial y} \right) + \frac{\partial}{\partial z} \left( (\nu + \nu_T) \frac{\partial v}{\partial z} \right) + f_{T,y} + f_{COR,y} \quad (2b)$$

$$u \frac{\partial w}{\partial x} + v \frac{\partial w}{\partial y} + w \frac{\partial w}{\partial z} = -\frac{1}{\rho} \frac{\partial p}{\partial z} + \frac{\partial}{\partial y} \left( (\nu + \nu_T) \frac{\partial w}{\partial y} \right) + \frac{\partial}{\partial z} \left( (\nu + \nu_T) \frac{\partial w}{\partial z} \right) + g\beta(\Theta - \Theta_0) + f_{T,z} + f_{COR,z} \quad (2c)$$

Here the Coriolis body force  $\mathbf{f}_{COR}$  is defined as

$$\mathbf{f}_{COR} = \mathbf{f}_c \times \mathbf{u}$$

where  $\mathbf{f}_c = -2\Omega(\sin \phi_{lat})\hat{\mathbf{z}}$ , the Earth's angular rotation rate is  $\Omega = 2\pi/T_{day}$ ,  $T_{day}$  is a sidereal day, and  $\phi_{lat}$  is the latitude of the location under consideration.

However, note that the inclusion of the Coriolis body force by itself results in only minor changes to the wake evolution for the cases considered here (see figure 1). The lack of any significant wake deflection is explained by the relatively large Rossby numbers ( $Ro = U_\infty/(f_c D) \sim 290 - 400$ ). This is consistent with the observations of Keck and Howland [5]). On the other hand, the inclusion of the veer profile, which is determined based on the LES precursor conditions, leads to noticeable wake skewing downstream.

3. **The wake models for comparison are too simple. The authors should compare their results to the WakeBlaster or the curled wake model. Also, given their focus on veer the authors should compare to the Gaussian model with the Abkar approach for veer (Abkar et al (2018)). Also, quantitative error metrics should be presented.**

We agree with the reviewer that a comprehensive comparison of models across many fidelity levels is desired and can help direct future efforts for improving wake models. However, in order for the results of such a comparison to be fairly presented, the models should be properly calibrated and tuned for the cases under consideration. Otherwise, the accuracy and capabilities of the wake comparisons may be clouded by inappropriate tuning.

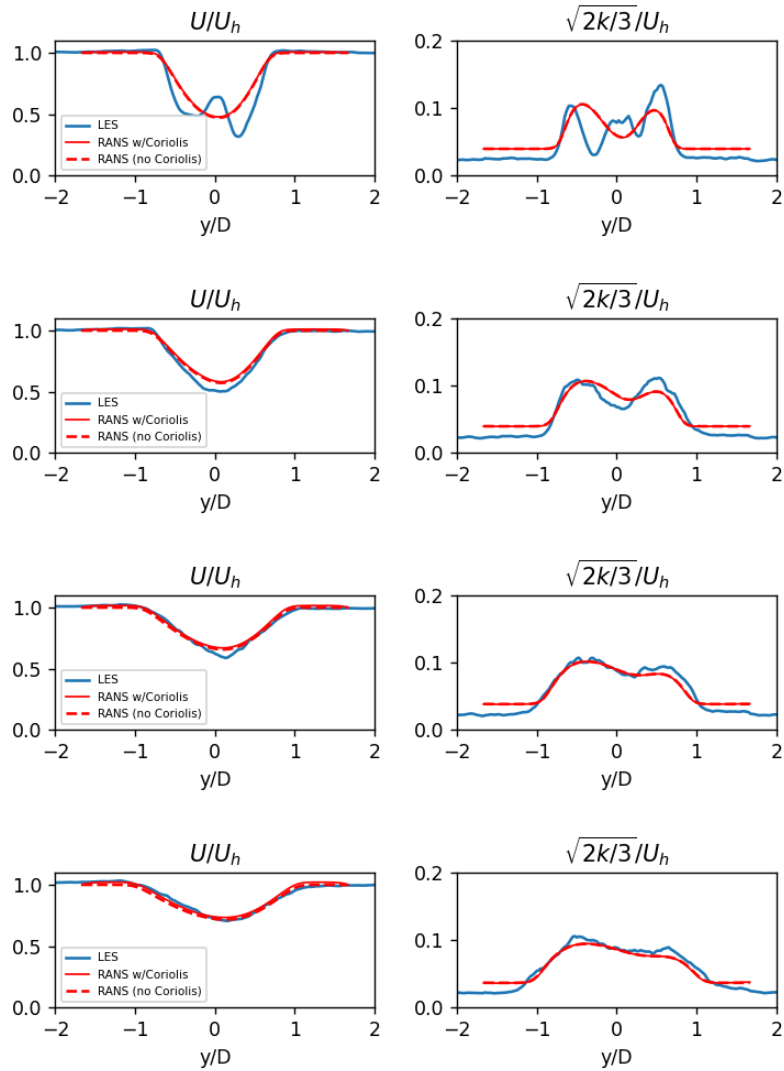


Figure 1: Comparison of the hub-height RANS wake and TKE profiles for the Med WS case, both wind and without Coriolis forcing.

While the calibration of additional wake models to the IEA15MW wind turbine and stable offshore conditions are not possible within the scope of the current study, the commonly used empirical Gaussian model was tuned for these cases as a part of a separate study [7]. This allowed for accurate comparisons between the RANS and FLORIS models where both models have been calibrated appropriately.

- 4. It appears that the RANS model is calibrated to the LES data and then compared back to the same LES data as validation. The RANS model must be compared to unseen test data. Some very brief comparisons are shown to a wind farm case but these comparisons are brief and not sufficiently quantitative. Additional unseen single turbine LES cases with different ABL conditions should be simulated and tested against the model.**

An additional case has been included in the updated manuscript where we demonstrate how the RANS model can be applied to an onshore wind turbine in a different inflow condition. Without changing the calibrations of  $C_\mu$ ,  $C_{1\epsilon}$ ,  $C_{2\epsilon}$  in section 2.5, and only adapting  $C_k$  for the ambient turbulence levels, the wake for a NREL5MW turbine in a 11.4 m/s slightly convective atmospheric boundary layer with no appreciable veer was reasonable well captured (see figures 2 and 3). The details behind this turbine and ABL setup are publicly available online<sup>1</sup> and on a Github repository<sup>2</sup>. The comparisons suggest that the calibrations have a reasonable large range of applicability, even though they were developed for large turbines in a stable offshore condition.

In future studies, more sophisticated actuator disk turbine models will be developed for this RANS method, which will allow for a wider range of wind speeds to be considered and even more general calibrations to be developed.

- 5. Section 2.2: The authors describe a boundary condition methodology which is something like a hybrid between wake modeling and RANS modeling approaches and must be more clearly explained and justified. Specifically, with a prescribed turbulence model and boundary conditions for  $k$  and  $\epsilon$ , this will imply a particular solution to the RANS equations with some velocity. However, the authors also claim they can achieve a “desired” veer profile. This is inconsistent. Any prescribed profile that is not the solution to the RANS & turbulence model combination at the inlet will evolve within the domain away from the prescribed profile, as is well established in RANS (Parente et al (2011) <https://doi.org/10.1016/j.jweia.2010.12.017>)**

In the updated manuscript, we have clarified that the inflow conditions described in section 2.2 require an additional input in order to establish the inlet veer profile, as Monin-Obukov theory does not provide this information. Multiple methods exist for determining the possible inflow profiles to the RANS method, including using the LES precursor profiles directly, or profiles generated from the output of another ABL solver. Future studies may examine such options, and this may allow the RANS model to consider more complicated profiles including inversion layer heights and low-level

---

<sup>1</sup><https://exawind.github.io/exawind-benchmarks/>

<sup>2</sup><https://github.com/Exawind/exawind-benchmarks/>

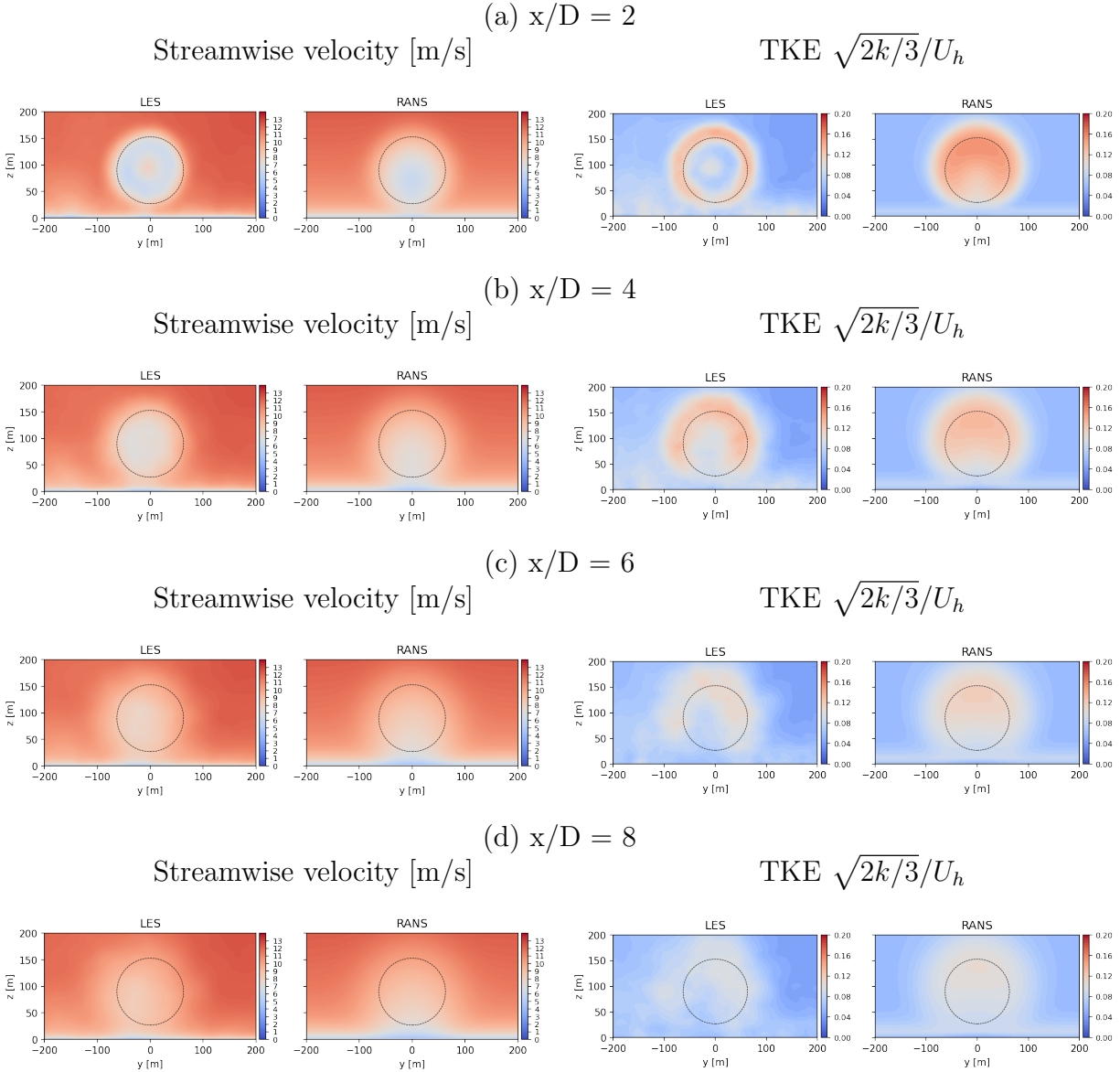


Figure 2: Comparison of the streamwise velocity and non-dimensional TKE for the NREL5MW turbine in a slightly convective inflow condition

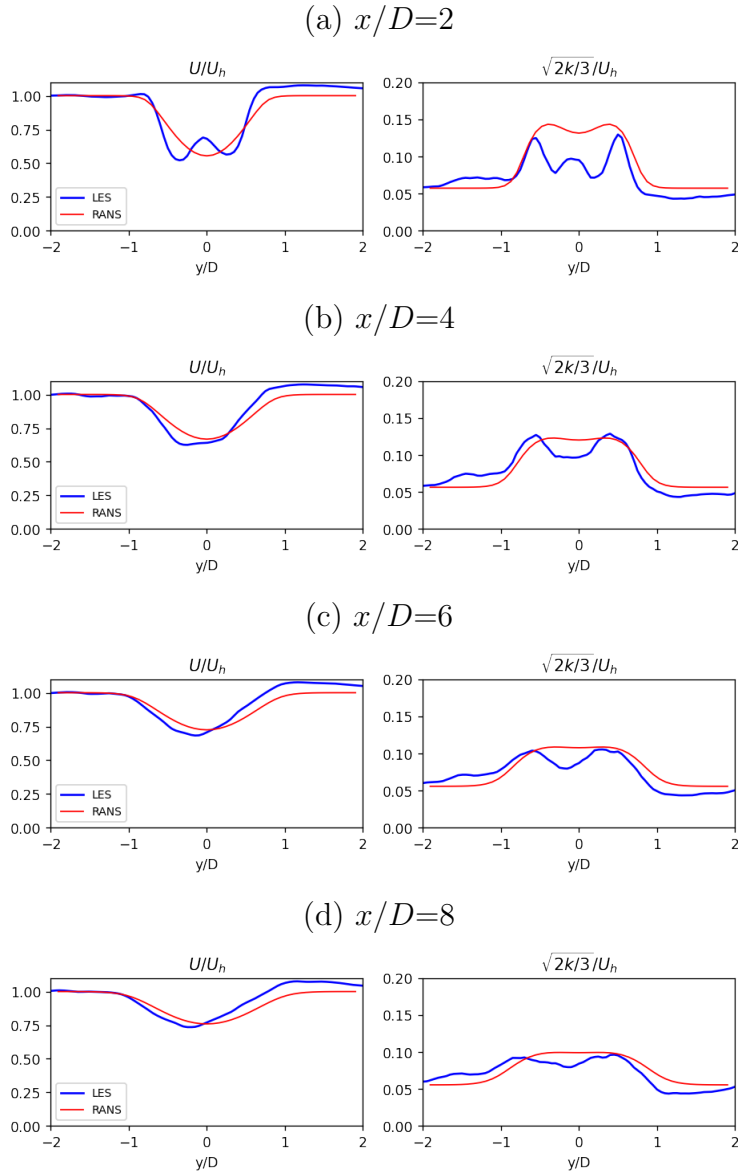


Figure 3: Comparisons of the normalized hub-height velocity and normalized TKE profiles between RANS and LES for the NREL5MW turbine in a slightly convective 11.4 m/s inflow condition.

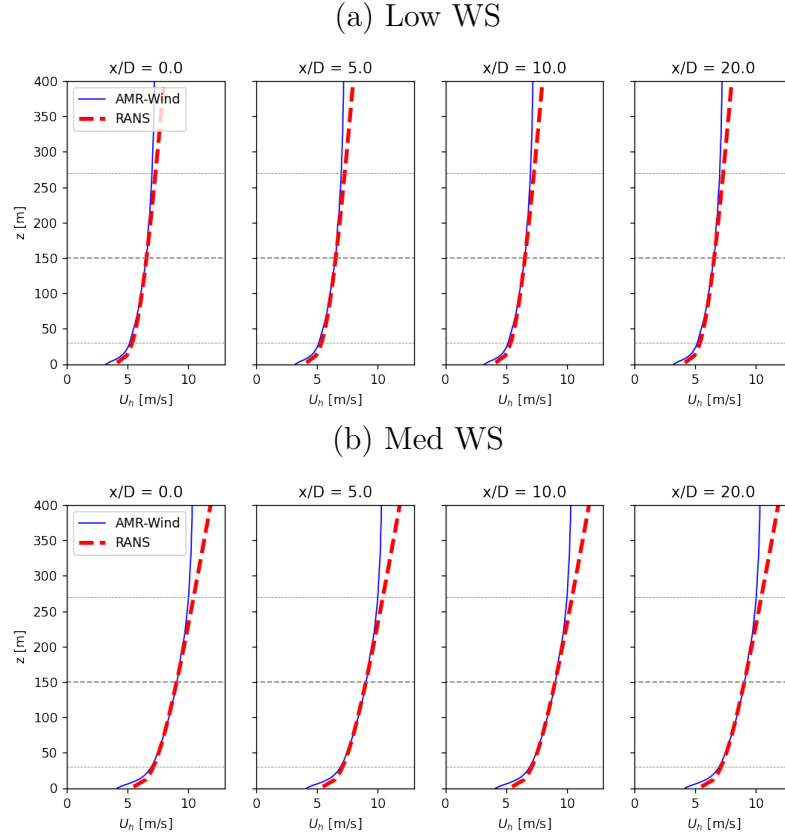


Figure 4: The streamwise evolution of the inflow profiles, without the presence of a turbine wake, for the (a) Low WS and (b) Med WS conditions over a distance of 20 diameters (4800 m).

jets. However, for the current work, the primary consideration is to establish a profile with the desired characteristics, and which is sufficiently close to the RANS solution that no significant evolution occurs before the first turbine. In tests where the inflow profiles were evolved without the presence of any turbine wake (Figure 4), the velocity profiles for the Low WS and Med WS cases were shown to have minimal changes over the span of 20D (4800 m).

## Minor comments

1. Line 5: “The full three-dimensional solution for the velocity, temperature, and turbulence variables are efficiently solved through an alternating direction implicit scheme that requires orders of magnitude less computational resources than traditional high fidelity approaches.”

The authors describe that their method is orders of magnitude cheaper than “high fidelity approaches” but it is not clear what approaches are referred to. Non-parabolic RANS or LES?

We have clarified this sentence in the abstract to specify that the higher fidelity ap-

proaches refer fully elliptic RANS or large-eddy simulations (LES).

2. **Line 30:** “More recent work (Narasimhan et al., 2022, 2025) has extended analytical wake models to include atmospheric shear and veer, but consistently accounting for these effects in interacting wakes or in the wake-added turbulence behavior remains an open question.”

Reference to original (Abkar et al (2018) <https://doi.org/10.3390/en11071838>) paper on wake modeling in shear and veer is absent.

In the introduction of the updated manuscript, we have included a reference to the work of Abkar et al [1].

3. **Line 49:** “This restricts the ability of the model to handle effects such as wake-ABL interactions or wake skewing and veering.”

The authors state that initializing the wakes in the velocity field, rather than a body forcing, restricts the ability to handle “wake-ABL interactions or wake skewing and veering.” This statement is not sufficient clear about what specific mechanisms cannot be handled by the velocity field approach. This must be rephrased to be clearer. Wake skewing and veering can be capturing via the velocity field (e.g. Abkar & Porte-Agel (2018)) and “wake-ABL interactions” is far too vague.

In the revised version of the manuscript, we have rephrased this section of the introduction to read:

“the turbine wakes are created by directly enforcing a deficit profile in the velocity solution rather than through body forces in the momentum equation itself. The solution of a single streamwise momentum equation also limits the ability of the model to handle effects such as wake-veer interactions or wake swirl interactions with the mean flow.”

This should clarify our intent, which is to point out that using enforced velocity profiles to create the turbine wakes in the combined curl model is more limiting than by using actuator disk forces, and solving only for the  $u$  variable limits the ability of the model to accurately capture swirl or veer impacts on wakes.

4. **Line 65:** “Previous studies have shown that the  $k-\epsilon$  model can accurately simulate stratified ABL conditions (Alinot and Masson, 2005), [...]”

I do not agree that the  $k-\epsilon$  model is accurate in stratified ABL conditions. This is too sweeping. It can be accurate, but has shown clear limitations as well (van der Laan et al (2017) <https://doi.org/10.1002/we.2017>)

In the section 2.1 of the updated manuscript, we have clarified that the  $k - \epsilon$  model of Alinot and Masson (2005) is applicable to the atmospheric surface layer, and has limitations as described in van der Laan et al [6]. We do not expect that the Monin-Obukhov profiles to apply in more complex situations with low level jets or above the atmospheric inversion height. However, in the tests of the formulation using the

IEA15MW reference turbine, the model was able to capture the flow accurately near the upper rotor tip locations.

We should note that the parabolized RANS formulation in this study is not limited to the  $k - \epsilon$  model, and can also be applied to other closure models. In future work we hope to explore other possibilities, including  $k - \omega$  SST [2] models or improving the current limitations of  $k - \epsilon$ , so that both the wake and the atmospheric are captured as accurately as possible.

- 5. Equations (1b)-(1d): The Coriolis forcing and geostrophic pressure gradient force are absent from these equations. This is concerning because the introduction motivated this paper by seeking to capture stratified ABL conditions and “veer.” This RANS model will not produce veer from Coriolis effects.**

The latest version of the manuscript clarifies the discussion of the forcing terms in the parabolic RANS model. To be consistent with the body forces used in the LES calculation, the Coriolis forcing terms are included. However, the Coriolis body forces by themselves play a negligible role in the dynamics of the turbine wake due to the high Rossby numbers, and the presence of veer is a larger factor in causing the wake skew (see response to question 3 above).

- 6. Line 98: “values of  $A_n$  are given in table 1 of Alinot and Masson (2005).” The 5 tunable parameters for  $A_n$  must be shown in this paper, not in a reference to a paper from 2005.**

In the revised version of the paper, the  $A_n$  parameters have been explicitly provided as table 1.

- 7. Equation 6: the authors solve a “parabolic” RANS equation that solves an elliptic pressure Poisson equation where propagation of forcing in  $x$  is neglected. This approximation of the Poisson equation to neglect  $x$ -derivatives may lead to major errors in the degree to which the induction is resolved by this model. This is a concern of this approach and must be tested in detail.**

A discussion of the parabolization process and pressure Poisson equation can be found in the response to main question 1 above.

- 8. Equation (19): this actuator disk model is not well posed for any simulation besides a single turbine, because the freestream velocity ( $U_\infty$ ) is not known in wind turbine arrays. Please clarify how this is done. Two turbine and wind farm cases are presented and  $U_\infty$  should not have been used to calculate  $C_T$  in the RANS model.**

In the updated version of the manuscript, this input to the actuator disk model has been clarified. The velocity used in the formula should be the upstream velocity  $U_{up}$ , and not the inflow velocity  $U_\infty$ , where  $U_{up}$  is computed using the rotor averaged velocity from the solution immediately upstream of the turbine location. This allows turbines

within a wind farm to respond to local, possibly waked, conditions without requiring knowledge of the undisturbed, far upstream  $U_\infty$  flow.

- 9. Section 3.1: AMR-Wind with ALM turbines are used for comparison. The actuator disk model should be used first, to eliminate the drivers of error from differences between uniformly loaded ADM and ALM, instead focusing on parabolised RANS vs. LES**

The reviewer’s comment raises an excellent point regarding the choices of turbine model fidelity and the best comparisons to be conducted for this study. We agree that a comparison of using an actuator disk model in the LES against the same actuator disk in the RANS study would remove any differences due to the turbine model itself. Indeed, there are many different choices of an actuator disk model, e.g., a uniformly loaded disk, a Joukowski actuator disk model, or a OpenFAST-coupled disk model, which could be appropriate for such a study.

However, one of the more unexpected findings of the current study was the fact that an actuator disk model is compatible with the parabolized RANS formulation itself, and that previous attempts to initialize the turbine wake by explicitly subtracting a wake deficit profile are unnecessary. This allows for a more natural method to handle partial turbine waking and an implementation of the turbine operation closer to that in the LES model. The results presented here demonstrate this proof-of-concept capability, and initial explorations have shown that more sophisticated actuator disk models are possible as well.

In the updated version of the manuscript, we have provided additional discussion on the available actuator disk models listed above, and the expected improvements once these are implemented.

- 10. Figure 6: The results seem to indicate that the initial wake magnitude is too weak in the parabolised RANS, and then the wake recovers too slowly. Again, the RANS was calibrated to the LES for  $x/D$  between 4 and 6. So the model is likely just overfit to agree well in these regimes, but will have the wrong wake recovery. This will cause large error outside of 4-6 D downwind.**

As an initial proof of concept for the calibration process, the streamwise locations were chosen based on the regions of interest for wakes in offshore wind farms, where lateral and streamwise turbine spacings are likely to be in the 4D-6D range. These calibration locations also avoid the near wake region  $x/D \leq 2$ , where the turbine model is unlikely to capture the flow immediately aft of the nacelle.

In future studies involving a larger number of conditions, both onshore and offshore wind turbines, and a wider range of wind speeds, the calibration process will likely broaden to include additional downstream locations and possibly other RANS parameters not considered here. This may improve the agreement of the wake model farther downstream compared to the current work.

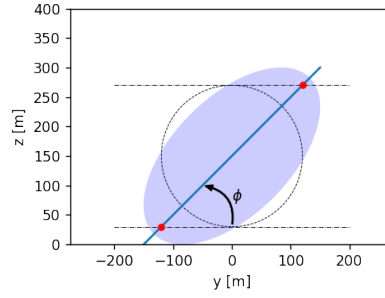
11. **Figure 8: The same results are seen, the wake is initially too weak, and then recovery is too slow. This would be clear if the velocity was plotted for all  $x$  values, similar to Figure 5 from Bastankhah (2014). The authors should make this plot for their comparisons with LES and other wake models.**

For the turbine wakes considered in the current study, looking at the evolution of the wake at single point (e.g., the centerline wake velocity deficit) may not provide a complete picture of the wake dynamics. However, one comparison of particular interest to this work is to examine the behavior of the wake skew angle in the different models. Here, the wake skew angle is calculated using the vertical angle of the wake’s major axis, as defined by the locations of the maximum wake deficit at the upper and lower rotor tip heights (Figure 5). As expected, this skew angle is nearly constant and close to  $90^\circ$  at all distances downstream for all of the FLORIS calculations. In the parabolic RANS approach, we see that the skew angles monotonically decrease in the downstream direction, and this trend is well captured when compared to the LES calculations for the Med WS case. The same trend is present in the Low WS case, although the RANS result is shifted compared to the LES. In the near wake region, both the RANS and LES begin with similar  $\phi$  angles, but a slower evolution of  $\phi$  is observed in the LES data between  $1D \leq x \leq 3D$ , resulting in an offset of approximately  $\Delta_\phi \approx [XYZ]$  degrees. The underlying reason behind this offset is still being investigated, but the overall trends are still present in the parabolized RANS model.

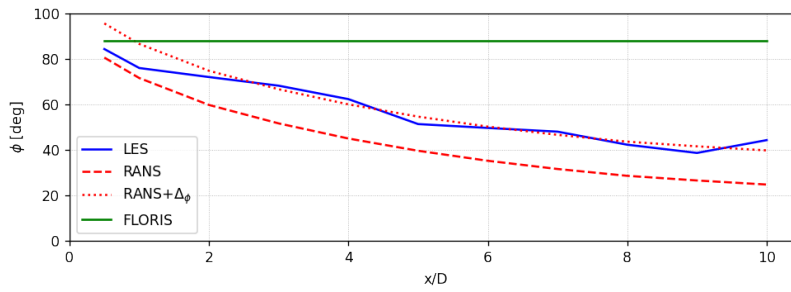
## References

- [1] Mahdi Abkar, Jens Norkaer Sorensen, and Fernando Porte-Agel. An analytical model for the effect of vertical wind veer on wind turbine wakes. *Energies*, 11(7), 2018.
- [2] Christiane Adcock, Marc Henry de Frahan, Jeremy Melvin, Ganesh Vijayakumar, Shreyas Ananthan, Gianluca Iaccarino, Robert D Moser, and Michael Sprague. Hybrid RANS-LES of the atmospheric boundary layer for wind farm simulations. In *AIAA SCITECH 2022 Forum*, page 1922, 2022.
- [3] Lawrence Cheung, Kenneth Brown, Philip Sakievich, Nathaniel deVelder, Thomas Herges, Daniel Houck, and Alan Hsieh. A Green’s function wind turbine induction model that incorporates complex inflow conditions. *Wind Energy*, n/a(n/a):e2956. e2956 we.2956.
- [4] Lawrence C Cheung and Sanjiva K Lele. Linear and nonlinear processes in two-dimensional mixing layer dynamics and sound radiation. *Journal of Fluid Mechanics*, 625:321–351, 2009.
- [5] Kirby S Heck and Michael F Howland. Coriolis effects on wind turbine wakes across neutral atmospheric boundary layer regimes. *Journal of Fluid Mechanics*, 1008:A7, 2025.
- [6] M. Paul van der Laan, Mark C. Kelly, and Niels N. Sørensen. A new k-epsilon model consistent with monin–obukhov similarity theory. *Wind Energy*, 20(3):479–489, 2017.

(a) Wake skew schematic



(b) Low WS



(c) Med WS

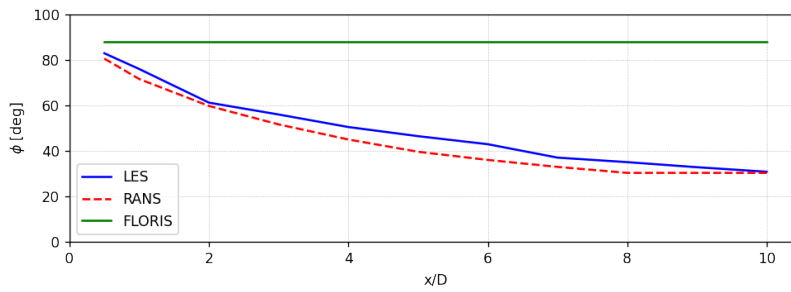


Figure 5: (a) Definition of the wake skew angle  $\phi$ . Downstream evolution of the wake skew  $\phi(x)$  for the (b) Low WS and (c) Med WS case.

- [7] Gopal R. Yalla, Kenneth Brown, Lawrence Cheung, Dan Houck, Nathaniel deVelder, and Balaji Jayaraman. Estimating annual energy production of wake mixing control strategies including comparisons to wake steering. *Wind Energy Science*, 2025.